Meson Decay in Invisibles ALPs

S. Rigolin[a,*] **and A.W.M. Guerrera**[a,b]

[a]*Department of Physics and Astronomy University of Padova and INFN Padova,*
Via Marzolo 8, Padova, Italy

[b]*Department of Physics and Astronomy University of Padova and INFN Padova,*
Via Marzolo 8, Padova, Italy

E-mail: stefano.rigolin@pd.infn.it,
alfredowaltermario.guerrera@studenti.unipd.it

Axion–Like–Particles are among the most economical and well motivated extensions of the Standard Model. In this talk ALP production from hadronic meson decays are presented. The general description of the hadronization techniques needed in order to calculate ALP emission in mesonic s– and t–channel tree–level processes is discussed, for pseudoscalar to pesudoscalar mesons. Accordingly, the decay amplitudes for $M_I \rightarrow M_F\, a$ are calculated. Finally, bounds on the (low–energy effective Lagrangian) ALP–fermion couplings are derived, from present and future flavor experiments.

*** FIXME: Name of conference, ***
*** FIXME: day-day Month YEAR ***
*** FIXME: Location, City, Country ***

---

[*]Speaker

---

1. Introduction

Light pseudoscalar particles are a common feature of many extensions of the Standard Model (SM) of particle physics. These can be naturally introduced in beyond SM (BSM) scenarios, following the QCD axion paradigm, as pseudo Nambu-Goldstone bosons (pGBs) of a global $U(1)_{PQ}$ symmetry, spontaneously broken at a scale $f_a \gg v$, with v denoting the SM Higgs vev. The main difference between the QCD axion and an Axion Like Particle (ALP) lies in abandoning the requirement that the only explicit breaking of the $U(1)_{PQ}$ symmetry arises from non–perturbative QCD effects [1], imposing the well known relation $m_a f_a \approx m_\pi f_\pi$. Therefore, allowing the ALP mass m_a and the PQ symmetry breaking scale f_a to be independent parameters gives rise to an abundance of scenarios populated by scalar singlets under the SM group, not necessarily tied to the solution of the Strong CP problem.

The most general CP conserving effective Lagrangian, including operators up to dimension five [2], and describing ALP interactions with SM fermions and gauge bosons, is given by:

$$\delta\mathcal{L}^a = -\frac{\partial_\mu a}{2f_a} \bar{f}\gamma^\mu (C_V + C_A \gamma^5) f - \frac{\partial_\mu a}{f_a} \sum_X c_X X^a_{\mu\nu} \tilde{X}^{\mu\nu a}, \tag{1}$$

where C_V and C_A are hermitian matrices in flavor space, a is the ALP field, f are the SM fermions and $X^a_{\mu\nu}$ indicates any SM gauge boson field strength, with $\tilde{X}^{\mu\nu a} \equiv X^a_{\alpha\beta}\epsilon^{\alpha\beta\mu\nu}/2$. Following most of the literature [3–8], a low–energy CP and flavor conserving effective Lagrangian for ALP-fermion interactions can be introduced:

$$\delta\mathcal{L}^a_{\text{ferm}} = -\frac{\partial_\mu a}{2f_a} c_i \, \bar{f}_i \gamma^\mu \gamma^5 f_i = i\frac{a}{f_a} m_i c_i \, \bar{f}_i \gamma^5 f_i + \dots . \tag{2}$$

The index i extends over all the fermions but the neutrinos, assumed to be massless, with c_i real, but not universal, ALP-fermions couplings. With the Lagrangian of Eq. (2) all flavor-violating effects will be loop induced and CKM suppressed, in the spirit of the Minimal Flavor Violation (MFV) ansatz.

ALP-fermions couplings can be studied in astro–particles/DM experiments or using astrophysical data, like for example supernova γ–ray emission. All these searches are, however, limited to very light ALP masses, rarely heavier than few keV, and, moreover, they can only bound first generation ALP-fermion couplings. Therefore, beam experiments are complementary in the exploration of the ALP couplings parameter space, and, among them, flavor factories are the most promising ones. Flavor physics experiments have received more and more attention from the phenomenological community [4, 6–11]. Strong limits on the ALP couplings in Eq. (1) can be derived, for example, through the study of the $K \to \pi a$ decay. In large part of the literature a flavor universal ALP–fermion coupling, $c_{a\Phi}$, is assumed. In this scenario, the $K \to \pi a$ amplitude is penguin dominated and one can bounds c_W and $c_{a\Phi}$ at the level of 10^{-3} for $f_a = 1$ TeV [4]. However, several models have been introduced where large hierarchies between axion couplings [12–14] are naturally produced. It is then of foremost phenomenological relevance to scan the ALP couplings parameter space following a less unbiased approach and to identify case by case which limits can be extracted from a given experiment on each independent ALP-fermion coupling.

However, one of the main obstacles in calculating hadronic observables is to deal with the associated non–perturbative matrix element. In treating transitions mediated by local operators,

like for example penguin contributions with heavy virtual particles in the loop, one can make use of the available Lattice QCD results [15]. Conversely, to compute products of bi–local operators mediated by virtual light states, alternative methods, like for example the Brodsky–Lepage technique [16–18], have to be used [7]. Only when the calculation of all these different contributions is done explicitly, one can fairly compare the sensitivity reach on ALP-fermion couplings of the different mesonic decay channels.

2.   Meson Hadronization in Flavor Changing Processes

Using the effective Lagrangian, implemented with the flavor conserving assumption, of Eq. 2 one can calculate the hadronic decay rates of mesons in ALPs. In the following, due to their experimental relevance, the pseudo-scalar meson hadronic decays:

$$K^+ \to \pi^+ a \qquad \text{and} \qquad K_L^0 \to \pi^0 a \tag{3}$$

will be mainly considered, with the ALP sufficiently long-living to escape the detector without decaying or decaying into invisible channels. In such a case the only possible ALP signature is its missing energy/momentum. The resulting formula can be easily adapted to describe general pseudoscalar to pseudoscalar meson decays into an invisible ALP, like for example $B_{s,d} \to K\,a$, $B_{s,d} \to \pi\,a$ by replacing the corresponding quark structures, decays constants and meson masses. For the general formula describing other type of hadronic meson decays in invisible ALPs (pseudoscalar to vector, vector to pseudoscalar and vector to vector) the reader is deferred to [11].

The processes of Eq. 3 receive contributions both from tree–level and one–loop diagrams. Typically, in these type of decays, the one–loop penguin diagrams with a top virtual exchange give the dominant contribution, as the $m_t/m_{q,ext}$ ratio largely compensate the loop suppression factor. The tree–level and one–loop decay channels involve, however, quite different hadronization structures that have to be properly taken into account for correctly comparing the relative contributions to the K decay rates as it will be briefly illustrated in the following sections.

2.1 The tree-level s-channel process

Charged pseudo-scalar meson decays proceed through the s–channel tree-level diagrams of Fig. 1. Here only the diagrams where the ALP is emitted from the K^+ meson are shown, the ones where the ALP is emitted from the π^+ follow straightforwardly. The tree-level diagram with the ALP emitted from the W^+ internal line automatically vanishes, being the WW-ALP coupling proportional to the fully antisymmetric 4D tensor. The hadronization of the s–channel can be done following the Lepage–Brodsky technique [16, 18]. Leptonic pseudo–scalar decays, $\mathcal{P} \to \ell\,\nu_\ell\,a$, deserve a similar treatment and have been derived in [3, 8, 19]. Let's recall briefly the notation.

The parent meson K^+ constituent quarks annihilate into a virtual W boson that then produces the final π^+ meson partons. The hadronic process can be factorized as

$$\langle \pi^+ | \, \bar{u}\,\Gamma_{(\pi)}\,d\,|0\rangle \, \langle 0| \, \bar{s}\,\Gamma_{(K)}\,u\,|K^+\rangle \tag{4}$$
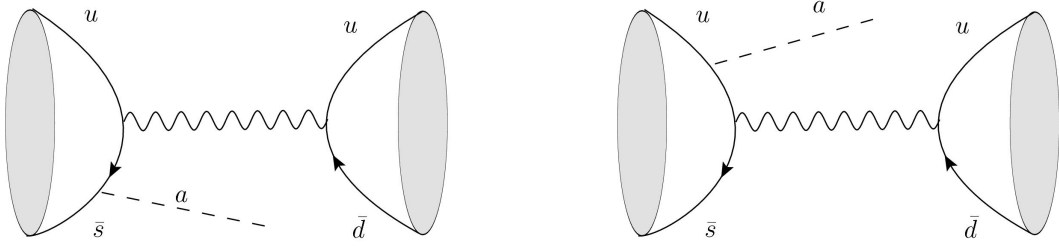
Figure 1: Tree level contributions to the $K^+ \to \pi^+ a$ amplitude, with the ALP emitted from the K^+ meson. Diagrams where the ALP is emitted from the π^+ quarks are straightforward.

with the operator insertion $\Gamma_{(\pi)} \otimes \Gamma_{(K)}$ being $\gamma^\mu P_L \otimes \Gamma_\mu$ or $\Gamma'_\mu \otimes \gamma^\mu P_L$ depending if the ALP is emitted by the initial or final mesons, with

$$\Gamma_\mu = \frac{4G_F}{\sqrt{2}} V_{us}^* V_{ud} \left(\frac{c_s \, m_s}{f_a} \gamma_5 \frac{\slashed{k}_a - \slashed{p}_{\bar{s}} + m_s}{m_a^2 - 2k_a \cdot p_{\bar{s}}} \gamma_\mu P_L - \frac{c_u \, m_u}{f_a} \gamma_\mu P_L \frac{\slashed{k}_a - \slashed{p}_u - m_u}{m_a^2 - 2k_a \cdot p_u} \gamma_5 \right) \tag{5}$$

$$\Gamma'_\mu = \frac{4G_F}{\sqrt{2}} V_{us}^* V_{ud} \left(\frac{c_u \, m_u}{f_a} \gamma_5 \frac{\slashed{k}_a + \slashed{p}'_u + m_u}{m_a^2 - 2k_a \cdot p'_u} \gamma_\mu P_L - \frac{c_d \, m_d}{f_a} \gamma_\mu P_L \frac{\slashed{k}_a + \slashed{p}'_{\bar{d}} - m_d}{m_a^2 - 2k_a \cdot p'_{\bar{d}}} \gamma_5 \right). \tag{6}$$

In Eqs. (5) and (6) with p_s, p_u and p'_d, p'_u the quark momenta of the initial and final meson are denoted, respectively, while the ALP momentum and mass are labelled as k_a and m_a.

To calculate the process amplitude one has to insert the Feynman amplitudes of Eqs. (5) and (6) inside the hadronic matrix element in Eq. 4. The vector and axial matrix elements can be parameterized in terms of the meson decay constants f_K and f_π as:

$$\langle 0| \, \bar{s} \, \gamma^\mu \, \gamma_5 \, u \, |K^+\rangle = i f_K P_K^\mu \qquad , \qquad \langle 0| \, \bar{s} \, \gamma^\mu \, u \, |K^+\rangle = 0 \tag{7}$$

$$\langle 0| \, \bar{d} \, \gamma^\mu \, \gamma_5 \, u \, |\pi^+\rangle = i f_\pi P_\pi^\mu \qquad , \qquad \langle 0| \, \bar{d} \, \gamma^\mu \, u \, |\pi^+\rangle = 0 \, . \tag{8}$$

To compute the $\langle 0| \, \bar{s} \, \Gamma_\mu \, u \, |K^+\rangle$ and $\langle \pi^+| \, \bar{u} \, \Gamma'_\mu \, d \, |0\rangle$ hadronic matrix elements, one has to assume a model for describing the effective quark–antiquark distribution inside the meson emitting the ALP. Following [3, 16, 18], the ground state of a meson M is parameterized with the wave–function

$$\Psi_M(x) = \frac{1}{4} \phi_M(x) \gamma^5 (\slashed{P}_M + g_M(x) M_M), \tag{9}$$

where P_M and M_M denote the momentum and the mass of the meson emitting the ALP. In Eq. (9), with x one typically denotes the fraction of the momentum carried by the heaviest quark in the meson. The function $\phi_M(x)$ describes the meson quarks momenta distribution, that for heavy and light mesons reads, respectively:

$$\phi_H(x) \propto \left[\frac{\xi^2}{1-x} + \frac{1}{x} - 1 \right]^{-2} \qquad , \qquad \phi_L(x) \propto x(1-x) \, , \tag{10}$$

with the normalization fixed such that:

$$\int_0^1 dx \, \phi_M(x) = 1. \tag{11}$$

4

The parameter ξ in $\phi_H(x)$ is a small parameter typically of $O(m_q/m_Q)$, being q and Q the light and heavy quark in the meson. The mass function $g_M(x)$ is usually taken to be a constant varying from $g_H(x) \approx 1$ and $g_L(x) \ll 1$ for a heavy or a light meson, respectively. The hadronic matrix element can then be obtained by integrating over the momentum fraction x the trace of the Γ^μ amplitude over the meson wave–function $\Psi_M(x)$:

$$\langle 0| \bar{Q}\, \Gamma^\mu\, q\, |M\rangle \equiv i f_M \int_0^1 dx \, \mathrm{Tr}\left[\Gamma^\mu \Psi_M(x)\right] . \tag{12}$$

By inserting Eqs. (5-6) into Eq. (12), and making the following assignments for the initial and final quark momenta:

$$
\begin{aligned}
p_{\bar{s}} &= x P_K & , && p_u &= (1-x) P_K \\
p'_{\bar{d}} &= x P_\pi & , && p'_u &= (1-x) P_\pi
\end{aligned}
$$

one obtains the following decay amplitudes for the K^+-ALP and π^+-ALP emission processes:

$$\mathcal{M}_{K^+} = \frac{G_F}{\sqrt{2}} (V_{us}^* V_{ud})\, f_K\, f_\pi\, (k_a \cdot P_\pi) \frac{M_K}{f_a} \times \tag{13}$$

$$\times \int_0^1 \left\{ \frac{c_s\, m_s\, \theta(x - \delta_a^K)}{m_a^2 - 2\, x\, k_a \cdot P_K} - \frac{c_u\, m_u\, \theta(1 - x - \delta_a^K)}{m_a^2 - 2\,(1-x)\, k_a \cdot P_K} \right\} \phi_K(x)\, g_K(x)\, dx$$

$$\mathcal{M}_{\pi^+} = \frac{G_F}{\sqrt{2}} (V_{us}^* V_{ud})\, f_K\, f_\pi\, (k_a \cdot P_K) \frac{M_\pi}{f_a} \times \tag{14}$$

$$\times \int_0^1 \left\{ \frac{c_d\, m_d\, \theta(x - \delta_a^\pi)}{m_a^2 - 2\, x\, k_a \cdot P_\pi} - \frac{c_u\, m_u\, \theta(1 - x - \delta_a^\pi)}{m_a^2 - 2\,(1-x)\, k_a \cdot P_\pi} \right\} \phi_\pi(x)\, g_\pi(x)\, dx$$

with $\delta_a^M = m_a^2/(2k \cdot P_M)$ an explicit cutoff introduced in the fractional momentum to remove the unphysical singularities appearing in the integrals.

To numerically evaluate the $K^+ \to \pi^+ a$ branching ratio one has to assume a specific form of the hadronic functions $\phi_K(x)$, $g_K(x)$, $\phi_\pi(x)$ and $g_\pi(x)$, and assign a low energy meaning to the quark masses. This, inevitably, introduces some model dependence in the calculation. To have an order of magnitude estimate of the $\mathcal{M}_{K^+}$ amplitude, one can consider the K-meson as a very light meson[1] (i.e. assuming an exact global $SU(3)$ symmetry), substituting the light quarks with the corresponding partons, i.e. $\hat{m}_s = \hat{m}_u = M_K/2$, one obtains, for a massless ALP:

$$\mathcal{M}_{K^+}^L \approx -\frac{3\, G_F\, f_K\, f_\pi}{4\sqrt{2}} (V_{us}^* V_{ud}) \frac{M_K^2}{f_a}\, g_K\, (c_s - c_u) . \tag{15}$$

A conservative estimate of the K/π ratio can be obtained by setting $g_\pi/g_K \approx M_\pi/M_K$, which predicts the following upper bound

$$R_{\pi K} = \left| \frac{\mathcal{M}_{\pi^+}}{\mathcal{M}_{K^+}} \right| \lesssim \left(\frac{M_\pi}{M_K} \right)^3 \simeq 1. \times 10^{-2} .$$

For this reason, even in the numerical calculation one can neglect the ALP-π emission as expected on a general ground, once same order ALP couplings to u, d and s quarks are assumed.

---

[1]For a more comprehensive discussion on this point the reader is deferred to Ref. [7].

Finally, from Eqs. (15) it appears evident the presence of an "accidental" cancellation if $c_s = c_u$ is assumed. This cancellation is still partially at work even when the full $\phi_K(x)$ is used and indicates a possible underestimation of the $\mathcal{M}_K$ amplitude (and consequently on the ALP-quark coupling limits) in a "universal" ALP–SM quark coupling scenario compared to the general case.

2.2 The tree-level t-channel process

Neutral pseudo-scalar meson decays proceed through the t–channel tree-level diagrams of Fig. 2. Here only the diagrams where the ALP is emitted from the K^0 meson are shown, the ones where the ALP is emitted from the π^0 follow straightforwardly. The tree-level diagram with the ALP emitted from the W^+ internal line automatically vanishes, as for the s–channel case. The hadronization of the t–channel can be done along the lines depicted in [16, 18].
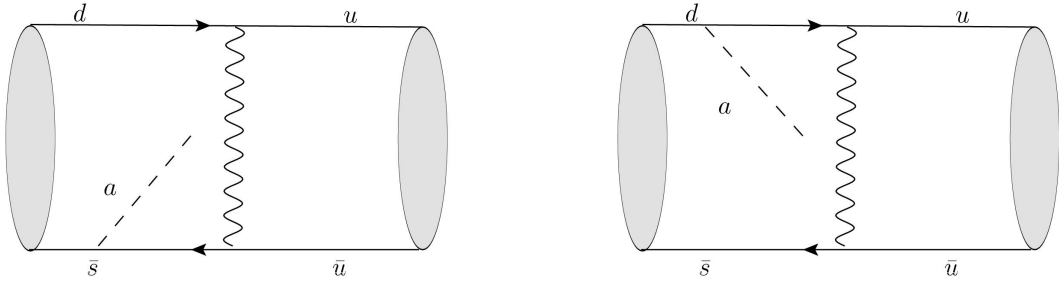
Figure 2: Tree level contribution to the amplitude for the $K^0 \to \pi^0 a$ decay, with the ALP emitted from the K^0 meson. Diagrams where the ALP is emitted from the π^0 quarks are straightforward. Similar diagrams can be depicted for the CP conjugate process $\bar{K}^0 \to \pi^0 a$.

Using the conventions defined in Eqs. (9) and (11), the neutral hadronic matrix element for the K^0 transition reads:

$$\langle \pi^0 | \, \Gamma_1 \otimes \Gamma_2 \, | K^0 \rangle \equiv -\frac{f_K f_\pi}{\sqrt{2}} \int_0^1 dx \int_0^1 dy \, \text{Tr} \left[\Psi_\pi(y) \Gamma_{(1)} \Psi_K(x) \Gamma_{(2)} \right] , \qquad (16)$$

with the $1/\sqrt{2}$ factor taking care of the Clebsch–Gordon suppression of the decay into the neutral π meson.

The operator insertion $\Gamma_{(1)} \otimes \Gamma_{(2)}$ is defined as $\gamma_\mu P_L \otimes \Gamma_{(\bar{q})}^\mu$ or $\Gamma_{(q)}^\mu \otimes \gamma_\mu P_L$ depending if the ALP is emitted from the $\bar{q}$ anti–quark (i.e. $\bar{s}$ for the K^0 and $\bar{u}$ for the π^0 meson) or from quark q (i.e. the d quark for the K^0 and the u quark for the π^0 meson), respectively, with

$$\Gamma_{(\bar{q})}^\mu = -\frac{4G_F}{\sqrt{2}} V_{us}^* V_{ud} \left(\frac{c_s m_s}{f_a} \gamma_5 \frac{\slashed{k}_a - \slashed{p}_{\bar{s}} + m_s}{m_a^2 - 2k_a \cdot p_{\bar{s}}} \gamma_\mu P_L - \frac{c_u m_u}{f_a} \gamma_\mu P_L \frac{\slashed{k}_a + \slashed{p}_{\bar{u}}' - m_u}{m_a^2 - 2k_a \cdot p_{\bar{u}}'} \gamma_5 \right) \quad (17)$$

$$\Gamma_{(q)}^\mu = -\frac{4G_F}{\sqrt{2}} V_{us}^* V_{ud} \left(\frac{c_d m_d}{f_a} \gamma_\mu P_L \frac{\slashed{p}_d - \slashed{k}_a + m_d}{m_a^2 - 2k_a \cdot p_d} \gamma_5 + \frac{c_u m_u}{f_a} \gamma_5 \frac{\slashed{k}_a + \slashed{p}_u' + m_u}{m_a^2 - 2k_a \cdot p_u'} \gamma_\mu P_L \right) \quad (18)$$

The $\bar{K}^0 \to \pi^0 a$ decay amplitude can be obtained similarly:

$$\langle \pi^0 | \, \bar{\Gamma}_1 \otimes \bar{\Gamma}_2 \, | \bar{K}^0 \rangle \equiv -\frac{f_K f_\pi}{\sqrt{2}} \int_0^1 dx \int_0^1 dy \, \text{Tr} \left[\Psi_\pi(y) \bar{\Gamma}_{(1)} \Psi_K(x) \bar{\Gamma}_{(2)} \right] , \qquad (19)$$

with the operator insertions $\bar{\Gamma}_{(1)} \otimes \bar{\Gamma}_{(2)}$ being $\gamma_\mu P_L \otimes \bar{\Gamma}^\mu_{(q)}$ or $\bar{\Gamma}^\mu_{(\bar{q})} \otimes \gamma_\mu P_L$ with

$$\bar{\Gamma}^\mu_{(q)} = -\frac{4G_F}{\sqrt{2}} V_{us} V^*_{ud} \left(\frac{c_s\, m_s}{f_a} \gamma_5 \frac{\not{p}_s - \not{k}_a + m_s}{m_a^2 - 2k_a \cdot p_s} \gamma_\mu P_L + \frac{c_u\, m_u}{f_a} \gamma_\mu P_L \frac{\not{k}_a + \not{p}'_u + m_u}{m_a^2 - 2k_a \cdot p'_u} \gamma_5 \right) \quad (20)$$

$$\bar{\Gamma}^\mu_{(\bar{q})} = -\frac{4G_F}{\sqrt{2}} V_{us} V^*_{ud} \left(\frac{c_d\, m_d}{f_a} \gamma_\mu P_L \frac{\not{k}_a - \not{p}_{\bar{d}} + m_d}{m_a^2 - 2k_a \cdot p_{\bar{d}}} \gamma_5 - \frac{c_u\, m_u}{f_a} \gamma_5 \frac{\not{k}_a + \not{p}'_{\bar{u}} - m_u}{m_a^2 - 2k_a \cdot p'_{\bar{u}}} \gamma_\mu P_L \right) \quad (21)$$

Adopting the same phase conventions as [20], one defines the neutral Kaon mass eigenstates:

$$K^0_{L,S} = \frac{1}{\sqrt{2(1+|\tilde{\epsilon}|^2)}} \left((1+\tilde{\epsilon})\, K^0 \pm (1-\tilde{\epsilon})\, \bar{K}^0 \right) \quad (22)$$

By making the following assignments for the initial and final quark momenta,

$$p_{\bar{s}} = x P_K \quad , \quad p'_u = (1-x)P_K$$
$$p_d = y P_\pi \quad , \quad p'_{\bar{u}} = (1-y)P_\pi$$

the amplitude for the $K^0_L \to \pi^0 a$ decay, when the ALP emitted by the K^0_L meson, reads:

$$\mathcal{M}_{K^0_L} = -\frac{\tilde{\epsilon}\, G_F}{2\sqrt{2}} \Re[V^*_{us}V_{ud}]\, f_{\bar{K}}\, f_\pi\, (k_a \cdot P_\pi) \frac{M_K}{f_a} \times$$
$$\times \int_0^1 \left\{ \frac{c_s\, m_s\, \theta(x - \delta^K_a)}{m_a^2 - 2x\, k_a \cdot P_K} - \frac{c_d\, m_d\, \theta(1-x-\delta^K_a)}{m_a^2 - 2(1-x)\, k_a \cdot P_K} \right\} \phi_K(x)\, g_K(x)\, dx \quad (23)$$

once the trivial integration in y is performed. As one can notice from Eq. (23), the amplitude for the K^0_L decay is proportional to the oscillation CP violation parameter $\tilde{\epsilon}$, as expected from general considerations on the CP properties of K^0 and $\bar{K}^0$ decays, and from the absence of imaginary part in the CKM for the tree–level diagram, i.e. $\Im[V^*_{us}V_{ud}] = 0$. Consequently the K^0_L decay amplitude is suppressed by $O(10^{-3})$, with respect to the corresponding tree–level charged process.

2.3 The one-loop process

Charged and neutral pseudo-scalar $K \to \pi a$ meson decays, assuming flavour conserving fermion-ALP interactions of Eq. (2), receive contributions at one–loop level[4, 9, 21] from the diagrams shown in Fig. 3. In the following only the contribution arising from fermion-ALP interaction will be considered.
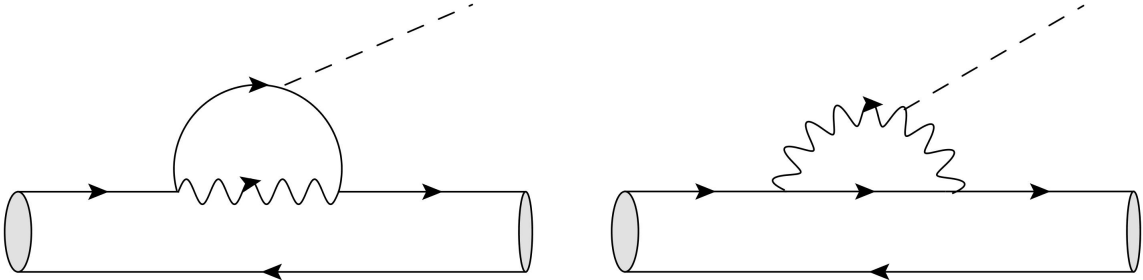

Figure 3: One-loop penguin contributions

In this kind of processes, only one quark line participate to the ALP emission, the other quark being a spectator. Customarily the hadronization of a matrix element between two pseudo-scalar meson mediated by a vector current, where one of the quark does not interact can be factorised as

$$\langle P| \bar{q}_1 \gamma^\mu Q_2 |M\rangle = f_+(q^2)(P_M + P_P)^\mu + f_-(q^2) q^\mu \tag{24}$$

with $q = P_M - P_P$. The form factors $f_{+,0}(0) = 1$ in the isospin symmetric limit, while the non approximated, q^2 dependent, form factors are obtained from LQCD calculation [15]. From Eq. (24) the amplitude for the $K^+ \to \pi^+ a$ decay reads:

$$\mathcal{M}^L_{K^+} = \frac{G_F m_t^2}{4\sqrt{2}\pi^2} (V_{ts}V^*_{td}) \frac{M^2_{K^+}}{f_a} \left(1 - \frac{M^2_{\pi^+}}{M^2_{K^+}}\right) \left[f_+(m_a^2) + \frac{m_a^2}{M^2_{K^+} - M^2_{\pi^+}} f_-(m_a^2)\right] \sum_{q=u,c,t} c^{(q)}_{sd} \tag{25}$$

with the coefficient

$$c^{(q)}_{sd} = \frac{V_{qi}V^*_{qj}}{V_{ts}V^*_{td}} \left[3 c_W \frac{g(x_q)}{x_t} - \frac{c_q x_q}{4 x_t} \ln\left(\frac{f_a^2}{m_q^2}\right)\right] \tag{26}$$

opportunely normalized in order to factorize out all the relevant scale dependences. The penguin with the ALP emitted from the internal W line is included for completeness, even if in the following phenomenological analysis $c_W = 0$ will be assumed. The dominant contribution from the penguin diagram is mostly proportional to the c_t coupling. For the K meson decay, with the charm contribution roughly accounting for 10% of the total contribution.

One-loop diagrams, with the ALP emitted from the initial/final quarks can be safely neglected being suppressed by at least a factor $m_s^2/m_W^2 \approx 10^{-6}$ with respect to the penguin contributions, as they arise at third order in the external momenta expansion. Therefore, no sensitivity on the ALP–down quark couplings can emerge in the $K \to \pi a$ decays from one loop diagrams.

An order of magnitude of the tree vs loop amplitude ratio is obtained from comparing Eqs. (15), giving:

$$R_{T/L} = \left|\frac{\mathcal{M}^T_{K^+}}{\mathcal{M}^L_{K^+}}\right| \approx 2 \pi^2 \frac{f_K f_\pi}{m_t^2} \left|\frac{V^*_{us} V_{ud}}{V^*_{ts} V_{td}}\right| \simeq 1. \times 10^{-2} . \tag{27}$$

showing the expected level of suppression. Even if the tree vs loop ratio is at the per cent level, the tree level diagrams may have a non negligible impact in the measurement of the $K \to \pi a$ decays, as in principle they depend on different and less constrained, down quark–ALP couplings.

Finally, the loop contribution to the $K^0_L \to \pi^0 a$ decay can be easily obtained from Eq. (25) and reads:

$$\mathcal{M}^{Loop}_{K^0_L} = \frac{G_F m_t^2}{4\sqrt{2}\pi^2} \Im(V_{ts}V^*_{td}) \frac{M^2_{K^+}}{f_a} \left(1 - \frac{M^2_{\pi^+}}{M^2_{K^+}}\right) \left[f_+(m_a^2) + \frac{m_a^2}{M^2_{K^+} - M^2_{\pi^+}} f_-(m_a^2)\right] c^{(t)}_{sd}$$

being proportional to the non vanishing imaginary part of the CKM matrix.

3. Bounds on ALP-fermion couplings from K meson decays

Armed with the tree–level and one–loop, charged and neutral, $K \to \pi a$ decays amplitudes obtained in the previous section, one can bound the ALP-fermion couplings using the experimental

limits provided by the NA62 [22, 23], E949 [24–26] and KOTO [27] experiments. The main assumption underlying the following phenomenological analysis is that the ALP lifetime is sufficiently long for escaping the detector (i.e. $\tau_a \gtrsim 100$ ps) or alternatively the ALP is mainly decaying in a, not better specified, invisible sector.

The tree–level amplitudes of Eqs. (13), (14) and (23) depend on the ALP couplings with s, d and u quarks, while the one–loop ones reported in Eqs. (25), (26) and (28), are typically dominated by the ALP coupling with the heaviest quark running in the loop, the t quark, being the c, u contributions suppressed by the $m_{u,c}/m_t$ mass ratio barring Cabibbo enhancements. Being the focus of this paper on ALP-fermion couplings, for the rest of the section $c_W = 0$ will be assumed. The interplay between the simultaneous presence of c_W and c_t has been discussed in detail in [4].

An analysis of the $K \rightarrow \pi a$ decay with completely general, but flavor conserving, ALP-quark couplings, would require to consider a five-parameters fit, $(c_u, c_d, c_c, c_s, c_t)$ beside the ALP mass m_a. In order to obtain meaningful information about the ALP-fermion couplings different simplifying assumptions have to be introduced. The phenomenological approach followed in this section will be twofold. First of all, in Sec. 3.1, all ALP-fermion couplings, introduced in the Lagrangian of Eq. (2), will be assumed independent. Then, using the tree–level amplitudes for the s– and t–channels, limits on (c_u, c_s) and (c_d, c_s) will be obtained, respectively, from the charged and neutral K meson decays, setting all the other ALP-quark couplings to 0. It should be emphasized that bounds on ALP-light quark couplings have been typically overlooked in the literature, where typically universal ALP–fermion couplings are assumed. Afterwards, in Sec. 3.2, only two independent family universal ALP-fermion couplings, $c_\uparrow$ for the up quarks and $c_\downarrow$ for the down ones, will considered, for sake of simplicity. Under this assumption, the interplay between the tree–level and loop contributions to the $K \rightarrow \pi a$ decay will be thoroughly discussed. Limits for the universal ALP–fermion coupling $c_{a\Phi}$ can be then obtained straightforwardly.

3.1 Tree–level Contributions

The tree–level amplitudes for charged and neutral K decays, given by Eq. (13) and (23) for charged and neutral channels respectively, in the most general case depend on four parameters: the ALP couplings to the three light quarks, c_u, c_d and c_s and the ALP mass, m_a. As derived in Eq. (16) the diagram with the ALP emitted by the pion contribution is strongly suppressed. Therefore, it seems reasonable, in the following, to neglect the π-ALP emission diagrams, and, consequently the K^+ decay rate depends only on the (c_u, c_s) ALP-fermion couplings, while the K^0 decay rates only on (c_d, c_s) ones.

The left plot in Fig. 4 shows the allowed regions of parameters as function of the ALP mass m_a for the chosen reference value $f_a = 1$ TeV. The shaded gray area is excluded by present experimental data. The upper and lower contours, delimiting the colored shaded area represent the bounds obtained setting $c_s = c_u$ and $c_s = -c_u$ respectively. The exclusive limit on c_s (c_u) with c_u (c_s) = 0 lies inside the colored shaded area. As noticed in Sec. 2, for $c_s = c_u$ the K^+ decay rate gets suppressed by an accidental parametric cancellation, leading to a less stringent bound on the ALP–fermion couplings. The shaded colored area represent consequently the typical uncertainty in the bound prediction from $K^+ \rightarrow \pi^+ a$ decay rates once letting the couplings (c_u, c_s) freely varying in the $|c_s/c_u| \leq 1$ range. The pink contours and shaded region are obtained from NA62 data [22, 23] while the cyan ones refer to bounds obtained from the E949 [24] experiment. For m_a
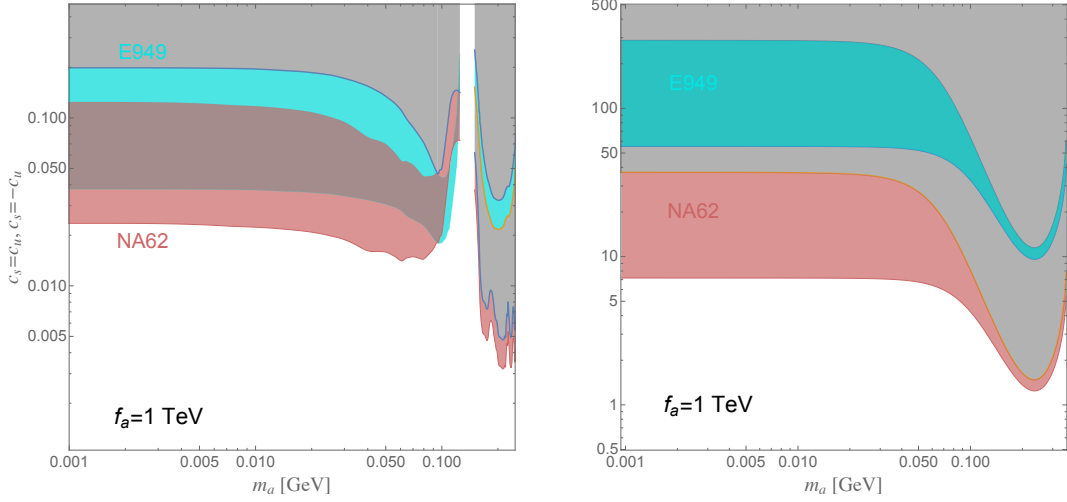
Figure 4: Excluded parameter regions derived from tree–level channels for charged (left) and neutral (right) $K \to \pi a$ decays. In the left–plot limits are derived from NA62 (pink) and E949 (cyan) experiments. In the right–plot, bounds are obtained from present (cyan) and expected (pink) KOTO data.

values below 0.15 GeV the two experiments provide similar results, with a slight edge in favor of NA62, bounding $(c_u, c_s) \lesssim 0.05$. In the $m_a > 0.15$ region, latest NA62 measurements has instead improved the sensitivity of E949 by roughly a factor 10, bounding $(c_u, c_s) \lesssim 0.01$. For $m_a \approx m_{\pi^0}$ both experiments loose sensitivity. No significative effects are obtained in this plot from the π-ALP emission diagrams, once the c_d parameter is assumed to lie in the perturbative range.

A similar analysis, for $K_L^0 \to \pi^0 a$ decay is presented in the right plot of Fig. 4, where the cyan and pink regions are obtained using the present[27] and expected KOTO experiment data, respectively. For this plot the upper and lower contours, delimiting the shaded area represent the bounds obtained setting on $c_s = c_d$ and $c_s = -c_d$ respectively. KOTO experiment results much less sensitive to the (c_d, c_s) ALP-fermion couplings, as CP violation in the tree–level processes can occurs only through the CP-mixing $\tilde{\epsilon}$ parameter, thus suppressing this channel by roughly a factor 10^{-3}. Present KOTO data do not provide any real constraint, with the prospect that future data could reach sensitivity to the perturbativity region[2].

The results showed in Fig. 4, even if not looking flashy, represent, nonetheless, the most stringent model–independent bounds on light quark couplings to ALP, for an ALP mass in the sub–GeV range, once flavour conserving, but not flavor universal ALP-fermion interactions, are assumed.

3.2 Interplay between tree–level and one–loop contributions

To constrain, simultaneously, tree–level and one–loop contributions to the $K \to \pi a$ decay one has to adopt simplified frameworks. Following [4], one can consider the scenario of universal ALP-quark coupling, $c_{a\Phi}$. From the analysis of Sec. 2 one easily realizes that in this scenario, the top-penguin loop contribution dominates the charged and neutral K decay, once $c_W = 0$ is assumed.

---

[2]Notice that KOTO experiment provides only mass independent limits on the $K_L^0 \to \pi^0 a$ branching ratio and consequently the loss of sensitivity in the $m_a \approx m_{\pi^0}$ region does not show up in the plot.
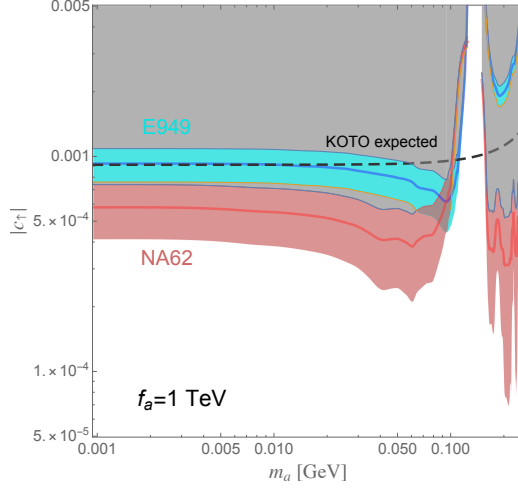
Figure 5: Excluded parameter regions for an universal ALP–up quark coupling $c_\uparrow$ derived from NA62 (pink), E949 (cyan) and KOTO expected (dashed line) experiments.
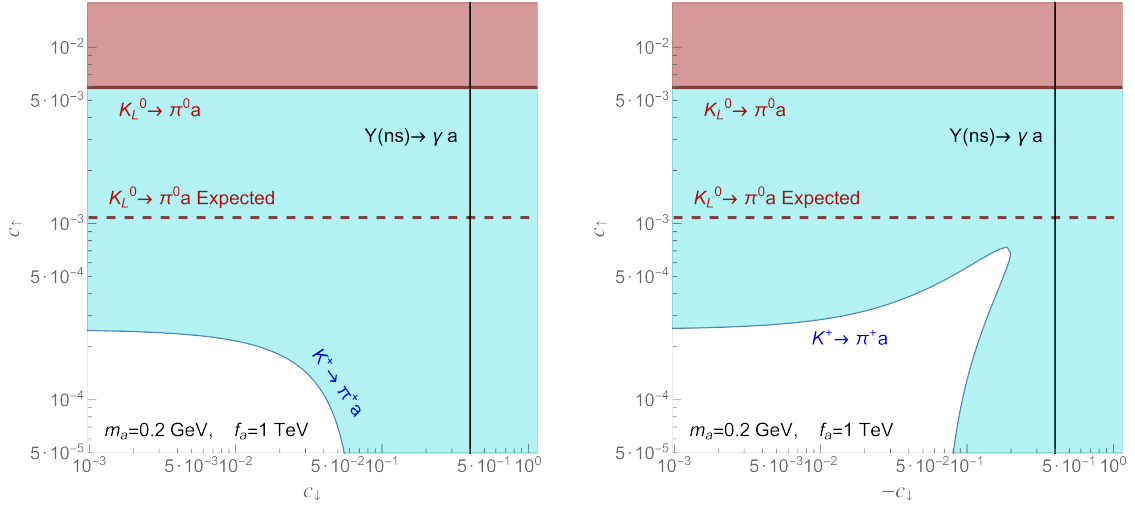
Figure 6: Excluded parameter regions for universal ALP–up and down quark couplings $c_\uparrow$ and $c_\downarrow$ derived from NA62 (cyan) and KOTO (pink and dashed pink line) and $Y(ns) \rightarrow \gamma a$ (full vertical black line) experiments. The left plot refer to the sign($c_\downarrow$) = sign($c_\uparrow$) case, while in the right one sign($c_\downarrow$) = −sign($c_\uparrow$) has been chosen.

The full cyan and pink lines in Fig. 5, represent the limits on $c_{a\Phi}$ obtained from E949 and NA62 respectively as function of the ALP mass m_a. The dashed gray line represents, instead, the $c_{a\Phi}$ limits from the expected KOTO upgrade. These results are in agreement with the bounds in [4] and show that K meson decays typically constrain $c_{a\Phi} \lesssim 10^{-3}$ in the sub-GeV ALP mass range.

In general MFV ALP frameworks, however, it may not be unconceivable to assign different, but flavor universal, PQ charges to the up and down quark sectors, see for example [28], that in the following will be denoted as $c_\uparrow$ and $c_\downarrow$, respectively. In this scenario, one–loop amplitudes only

depend from $c_\uparrow$ while the tree–level amplitudes are practically proportional to a linear combination of $c_\uparrow$ and $c_\downarrow$, as evident for example in the simplified amplitudes of Eqs. (15). From the tree–level analysis, summarized in Fig. 4, one learns that present data limit $c_\downarrow$ to be typically below 10^{-1}. Indeed, to study the interplay between tree–level and one–loop the reference value $c_\downarrow = \pm 0.05$ has been chosen, somehow in the ridge of the parameters allowed from the previous analysis on tree–level contributions. The blue and brown shaded regions showed in Fig. 5 represent the variability of NA62 and E979 bounds on $c_\uparrow$ once $c_\downarrow$ is let varying in the $[-0.05, 0.05]$ range. The presence of the tree-level contribution can modify the bounds on $c_\uparrow$ extracted from penguin diagrams of roughly one order of magnitude, in all the m_a range. The expected KOTO limits on the $K_L^0 \to \pi^0 a$ decay is reported in Fig. 5 as a black dashed line, giving a practically constant bound $c_\uparrow \lesssim 1 \times 10^{-3}$ over all the m_a range of interest, yet not competitive with the charged sector one.

Finally, in Fig. 6, a summary on the combined bounds on $(c_\uparrow, c_\downarrow)$ is presented for two reference values of the ALP mass $m_a = 0\,\text{GeV}$ and $m_a = 0.2\,\text{GeV}$. For the two upper plots $\text{sign}(c_\downarrow) = \text{sign}(c_\uparrow)$ has been taken. In the lower plots, where $\text{sign}(c_\downarrow) = -\text{sign}(c_\uparrow)$ has been considered, a partial cancellation between one–loop and tree-level contributions takes place. In this second scenario, the $c_\downarrow$ constraint from the $\Upsilon(ns)$ decays at Babar and Belle (full vertical black line) derived by [5] can contribute to close this flat direction.

4. Bounds on ALP-fermion couplings from D and B meson decays

Very promising results are expected in a near future from D and B pseudoscalar meson decays in invisible ALPs, especially from B–factories [4, 6, 9, 11]. The analysis done in the previous section can be easily extended to heavier pseudoscalar meson decays simply replacing the corresponding valence quarks. For example Eqs. 5 and 6 can be generalize substituting the K-meson quarks $\bar{s}(u) \to \bar{Q}(q)$ and the π-meson quarks $\bar{d}(u) \to \bar{Q}'(q')$. In Tab. 1 the amplitudes of several charged and neutral pseudoscalar meson decays are collected. For definiteness, $m_a = 0$, $f_a = 1$ TeV and $c_f = \pm 1$ have been used. As noticed in Eqs. (15) accidental cancellation can occurs in the tree–level amplitudes, depending on the relative sign between $c_{Q^{(\prime)}}$ and $c_{q^{(\prime)}}$. To make evident the impact of this accidental cancellation, the tree-level results in Tab. 1 has been shown with a $(min - max)$ interval, obtained by setting $c_{Q^{(\prime)}}/c_{q^{(\prime)}} = (+1, -1)$ respectively. From the results of Tab. 1, one learns which is the effectiveness of this parametric cancellation. Depending on the specific decay channel, the tree-level decay rate can change from one to two orders of magnitude.

It is also useful to note that the ratio between the tree-level ISR and FSR amplitudes is always independent of the particular nature of the decay (s or t) and is given by:

$$R_{I/F}^T = \left| \frac{\mathcal{M}_I^{(s,t)}}{\mathcal{M}_F^{(s,t)}} \right| \simeq \left(\frac{M_I}{M_F} \right)^2, \tag{28}$$

with the identity strictly holding in the ALP massless limit and assuming a "very light" or a "very heavy" DA function. Therefore, for all the corresponding processes, the decay amplitude is always dominated by the ISR ALP emission. Finally, in Tab. 1, both the tree-level and penguin contributions, when available, are presented. As a rule of thumb the tree-level vs one-loop amplitudes ratio

Channel	Tree–Level	Penguin
$B_c^\pm \to D_s^\pm a$	$(6 - 160) \times 10^{-11}$	2×10^{-6}
$B_c^\pm \to D^\pm a$	$(1 - 30) \times 10^{-11}$	3×10^{-7}
$B_c^\pm \to K^\pm a$	$(8 - 230) \times 10^{-12}$	n.a.
$B_c^\pm \to \pi^\pm a$	$(3 - 85) \times 10^{-11}$	n.a.
$B^\pm \to D_s^\pm a$	$(5 - 30) \times 10^{-12}$	n.a.
$B^\pm \to D^\pm a$	$(1 - 7) \times 10^{-12}$	n.a.
$B^\pm \to K^\pm a$	$(8 - 50) \times 10^{-13}$	2×10^{-6}
$B^\pm \to \pi^\pm a$	$(3 - 20) \times 10^{-12}$	3×10^{-7}
$D_s^\pm \to K^\pm a$	$(6 - 300) \times 10^{-12}$	7×10^{-12}
$D_s^\pm \to \pi^\pm a$	$(2 - 120) \times 10^{-11}$	n.a.
$D^\pm \to K^\pm a$	$(1 - 50) \times 10^{-12}$	n.a.
$D^\pm \to \pi^\pm a$	$(5 - 200) \times 10^{-12}$	6×10^{-12}
$K^\pm \to \pi^\pm a$	$(2 - 10) \times 10^{-12}$	5×10^{-10}
$B_s^0 \to D_s^0 a$	n.a.	4×10^{-7}
$B_s^0 \to D^0 a$	$(7 - 70) \times 10^{-12}$	n.a.
$B_s^0 \to K_L^0 a$	n.a.	3×10^{-7}
$B^0 \to D^0 a$	$(3 - 30) \times 10^{-11}$	n.a.
$B^0 \to K_L^0 a$	n.a.	4×10^{-6}
$B^0 \to \pi^0 a$	$(1 - 10) \times 10^{-12}$	5×10^{-7}
$D^0 \to K_L^0 a$	$(7 - 270) \times 10^{-13}$	n.a.
$D^0 \to \pi^0 a$	$(2 - 100) \times 10^{-12}$	3×10^{-12}
$K_L^0 \to \pi^0 a$	$(4 - 20) \times 10^{-15}$	1×10^{-10}

Table 1: Tree-level and penguin contribution to the hadronic charged meson decay rates, calculated for $m_a = 0$, $f_a = 1$ TeV and $c_f = \pm 1$, expressed in GeV^{-1} units. The interval in the tree–level column is obtained by setting $c_Q/c_q = (1, -1)$.

can be estimated by:

$$R_{T/L} = \left| \frac{\mathcal{M}_{\mathrm{T}}^{(s,t)}}{\mathcal{M}_{\mathrm{L}}} \right| \approx 2\,\pi^2\, \frac{f_I\, f_F}{m_f^2} \left| \frac{V_{\mathrm{T}}^{\mathrm{CKM}}}{V_{\mathrm{L}}^{\mathrm{CKM}}} \right|, \tag{29}$$

where m_f is the mass of the heaviest quark running in the penguin and $f_{I,F}$ the initial and final meson decay constants. Notice that for most of the D decays the tree-level contribution is comparable if not larger than the loop one, as clearly the m_b^2 penguin loop enhancement is not sufficient to compensate for the typical loop suppression factor. Conversely, for the K and B meson sector the tree/loop ratio looks really tiny thanks to the large m_t^2 penguin enhancement. Nevertheless, for the K sector the tree-level diagrams may have a non negligible impact, as they depend on different, and often less constrained, ALP-fermion couplings, as discussed in the previous section.
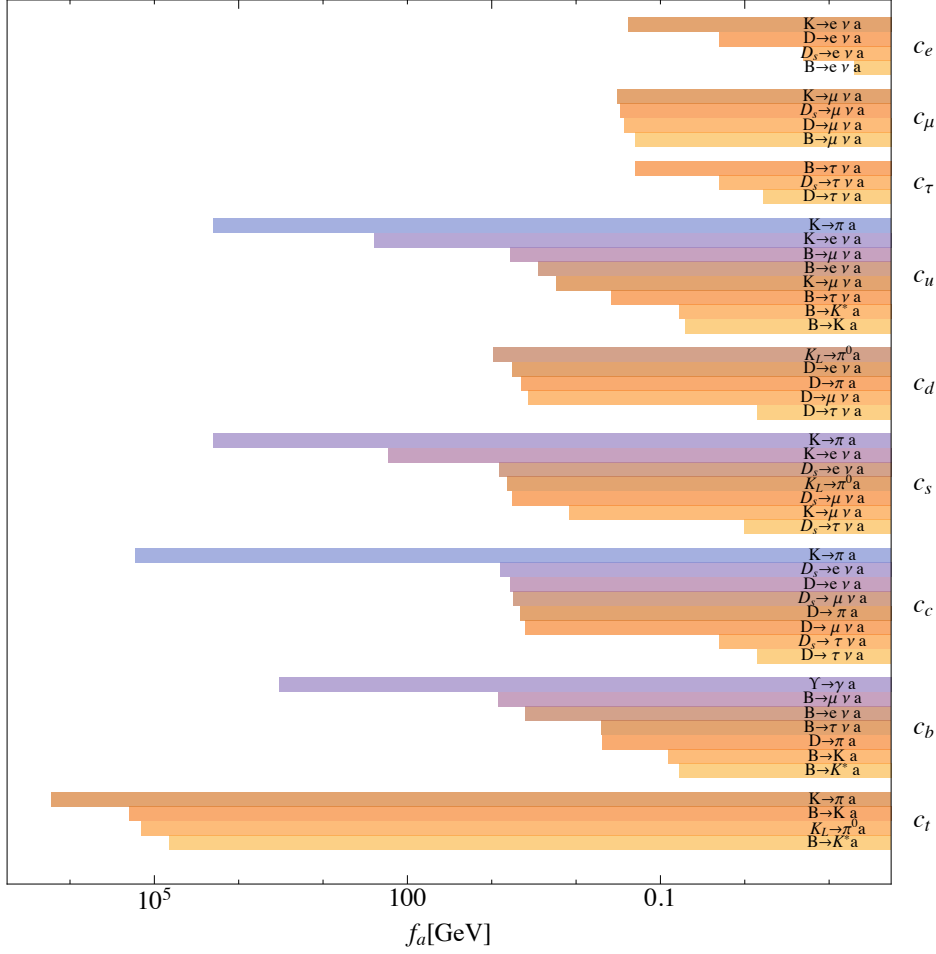
Figure 7: Bounds on f_a (expressed in GeV) obtained from meson decays into an invisible ALP, for $m_a = 0$ and assuming the corresponding $c_i = 1$, while setting all the other couplings to 0.

4.1 Phenomenological Summary

Finally, a comprehensive summary of all the bounds on flavor conserving ALP–fermion couplings derived in the previous section is presented in Fig. 7. To be able to fairly compare all the different analysis, the limits on the $U(1)_{PQ}$ breaking scale f_a (expressed in GeV) are shown, for $m_a = 0$ and by assuming the corresponding $c_i = 1$, with all the other couplings set to 0. Therefore, the f_a value plotted represents the highest energy scale tested, at present, in each decay channel. One can notice that the most stringent bounds on f_a come from the top sector, trough the m_t enhanced penguin contributions [4, 7]. From K and B hadronic pseudoscalar meson decays one tests $f_a \simeq (10^5 - 10^6)$ GeV. This is the lowest energy scale at which new physics in the ALP sector may appear, when a universal ALP-fermion coupling is assumed. $K \to \pi a$ decay provides the strongest bounds for all the ALP-quark couplings in the non-universal, but flavor conserving ALP-fermion scenario, with the only exception of the ALP-bottom coupling where the strongest bound comes from the $\Upsilon(ns) \to \gamma a$ decay [5]. Bounds on $c_{t,c}$ enter from the penguin loop diagram, while bounds on $c_{u,d,s}$ are due to the tree-level amplitude contribution. Meson leptonic decays produces

14

an upper bound on $f_a \simeq (10^{-1} - 10)$ GeV in the ALP-lepton sector.

5. Acknowledgements

References

[1] Steven Weinberg. A new light boson? *Phys. Rev. Lett.*, 40:223–226, Jan 1978.

[2] Howard Georgi, David B. Kaplan, and Lisa Randall. Manifesting the Invisible Axion at Low-energies. *Phys. Lett. B*, 169:73–78, 1986.

[3] Y.G. Aditya, Kristopher J. Healey, and Alexey A. Petrov. Searching for super-WIMPs in leptonic heavy meson decays. *Phys. Lett. B*, 710:118–124, 2012, arXiv: 1201.1007 [hep-ph].

[4] M.B. Gavela, R. Houtz, P. Quilez, R. Del Rey, and O. Sumensari. Flavor constraints on electroweak ALP couplings. *Eur. Phys. J. C*, 79(5):369, 2019, arXiv: 1901.02031 [hep-ph].

[5] L. Merlo, F. Pobbe, S. Rigolin, and O. Sumensari. Revisiting the production of ALPs at B-factories. *JHEP*, 06:091, 2019, arXiv: 1905.03259 [hep-ph].

[6] Jorge Martin Camalich, Maxim Pospelov, Pham Ngoc Hoa Vuong, Robert Ziegler, and Jure Zupan. Quark Flavor Phenomenology of the QCD Axion. *Phys. Rev. D*, 102(1):015023, 2020, arXiv: 2002.04623 [hep-ph].

[7] Alfredo Walter Mario Guerrera and Stefano Rigolin. Revisiting $K \to \pi a$ decays. *Eur. Phys. J. C*, 82(3):192, 2022, arXiv: 2106.05910 [hep-ph].

[8] Jorge Alda Gallo, Alfredo Walter Mario Guerrera, Siannah Peñaranda, and Stefano Rigolin. Leptonic meson decays into invisible ALP. *Nucl. Phys. B*, 979:115791, 2022, arXiv: 2111.02536 [hep-ph].

[9] Eder Izaguirre, Tongyan Lin, and Brian Shuve. Searching for Axionlike Particles in Flavor-Changing Neutral Current Processes. *Phys. Rev. Lett.*, 118(11):111802, 2017, arXiv: 1611.09355 [hep-ph].

[10] Martin Bauer, Matthias Neubert, Sophie Renner, Marvin Schnubel, and Andrea Thamm. Flavor probes of axion-like particles. *JHEP*, 09:056, 2022, arXiv: 2110.10698 [hep-ph].

[11] Alfredo Walter Mario Guerrera and Stefano Rigolin. ALP production in weak mesonic decays. *Fortsch. Phys.*, 2023:2200192, 11 2022, arXiv: 2211.08343 [hep-ph].

[12] Kiwoon Choi, Hyungjin Kim, and Seokhoon Yun. Natural inflation with multiple sub-Planckian axions. *Phys. Rev. D*, 90:023545, 2014, arXiv: 1404.6209 [hep-th].

[13] David E. Kaplan and Riccardo Rattazzi. Large field excursions and approximate discrete symmetries from a clockwork axion. *Phys. Rev. D*, 93(8):085007, 2016, arXiv: 1511.01827 [hep-ph].

[14] Gian F. Giudice and Matthew McCullough. A Clockwork Theory. *JHEP*, 02:036, 2017, arXiv: 1610.07962 [hep-ph].

[15] N. Carrasco, P. Lami, V. Lubicz, L. Riggio, S. Simula, and C. Tarantino. $K \to \pi$ semileptonic form factors with $N_f = 2 + 1 + 1$ twisted mass fermions. *Phys. Rev. D*, 93(11):114512, 2016, arXiv: 1602.04113 [hep-lat].

[16] G.Peter Lepage and Stanley J. Brodsky. Exclusive Processes in Perturbative Quantum Chromodynamics. *Phys. Rev. D*, 22:2157, 1980.

[17] Stanley J. Brodsky and G. Peter Lepage. Large Angle Two Photon Exclusive Channels in Quantum Chromodynamics. *Phys. Rev. D*, 24:1808, 1981.

[18] Adam Szczepaniak, Ernest M. Henley, and Stanley J. Brodsky. Perturbative {QCD} Effects in Heavy Meson Decays. *Phys. Lett. B*, 243:287–292, 1990.

[19] Derek E. Hazard and Alexey A. Petrov. Lepton flavor violating quarkonium decays. *Phys. Rev. D*, 94(7):074023, 2016, arXiv: 1607.00815 [hep-ph].

[20] Andrzej J. Buras. Weak Hamiltonian, CP violation and rare decays. hep-ph/9806471, arXiv: hep-ph/9806471.

[21] Martin Bauer, Matthias Neubert, and Andrea Thamm. Collider Probes of Axion-Like Particles. *JHEP*, 12:044, 2017, arXiv: 1708.00443 [hep-ph].

[22] Eduardo Cortina Gil et al. Search for a feebly interacting particle X in the decay $K^+ \to \pi^+ X$. *JHEP*, 03:058, 2021, arXiv: 2011.11329 [hep-ex].

[23] Eduardo Cortina Gil et al. Measurement of the very rare $K^+ \to \pi^+ \nu \bar{\nu}$ decay. arXiv 2103.15389, arXiv: 2103.15389 [hep-ex].

[24] A. V. Artamonov et al. Study of the decay $K^+ \to \pi^+ \nu \bar{\nu}$ in the momentum region $140 < P_\pi < 199$ MeV/c. *Phys. Rev. D*, 79:092004, 2009, arXiv: 0903.0030 [hep-ex].

[25] A.V. Artamonov et al. New measurement of the $K^+ \to \pi^+ \nu \bar{\nu}$ branching ratio. *Phys. Rev. Lett.*, 101:191802, 2008, arXiv: 0808.2459 [hep-ex].

[26] S. Adler et al. Measurement of the K+ –> pi+ nu nu branching ratio. *Phys. Rev. D*, 77:052003, 2008, arXiv: 0709.1000 [hep-ex].

[27] J.K. Ahn et al. Search for the $K_L \to \pi^0 \nu \bar{\nu}$ and $K_L \to \pi^0 X^0$ decays at the J-PARC KOTO experiment. *Phys. Rev. Lett.*, 122(2):021802, 2019, arXiv: 1810.09655 [hep-ex].

[28] L. Merlo, F. Pobbe, and S. Rigolin. The Minimal Axion Minimal Linear σ Model. *Eur. Phys. J. C*, 78(5):415, 2018, arXiv: 1710.10500 [hep-ph]. [Erratum: Eur.Phys.J.C 79, 963 (2019)].